

Experimental Demonstration and Simulation of a Dual-Stage Solid Propellant Gun Concept

Boaz Brill,* Shlomo Wald,* David Kimchi,* and Zvi Kaplan*
Soreq Nuclear Research Center, Yavne 70600, Israel

A novel method for the acceleration of projectiles to hypervelocity is presented. The method utilizes two solid grain propellant charges which are operated in tandem in a dual-stage mode. The second charge is encapsulated into a massive case which is placed adjacent to the projectile. This stage is ignited at a time delay, after the first charge. Experiments done on a 13-mm barrel demonstrate the feasibility of this acceleration scheme. Zero-dimensional simulations predict significant improvement over single-stage gun, using the same maximal pressure as imposed by conventional barrels. A specific calculation of a 0.48-kg projectile accelerated in a 4.4-m-long, 60-mm barrel predicts velocities over 2500 m/s.

Nomenclature

A	= barrel cross-sectional area
C_1, C_2	= mass of main charge and moving charge
l	= $y_2 - y_1$, the distance between m_2 and m_1
m_1, m_2	= masses of the dynamic breech and the projectile, respectively
P_{air}	= air pressure in front of the projectile
$P1-P7$	= measured pressures in successive locations along the barrel, $P1$ = at the breech
P_1, P_2	= average pressures in the two gas media, 1 = main, 2 = moving charge
P_{1b}, P_{2b}	= pressures behind the dynamic breech and at the projectile base
P_{1c}, P_{2c}	= breech pressures
y_i, v_i, a_i	= coordinate, velocity, and acceleration of m_i , $i = 1, 2$

I. Introduction

THE quest for ever faster projectiles has driven generations of engineers since the invention of ballistics. In terms of kinetic energy, the efficiency of current guns is very close to the theoretical limits and any improvement requires a significant upgrading with only diminishing returns. In the last decade it has become widely accepted that it will be very hard to accommodate future needs using conventional ballistics.

The major limitation of conventional ballistics that prevents attaining high velocities is rarefaction. It stems from the fact that while accelerating the projectile the propellant gases accelerate too. As a result, significant pressure gradients develop along the barrel's axis and the pressure at the projectile base becomes significantly smaller than that at the breech. The maximal velocities that can be efficiently attained using conventional ballistics are therefore limited to somewhat higher than the speed of sound in the accelerating medium.

In the last few years several alternative acceleration techniques have been extensively investigated. Some of them, like the rail-gun,¹ need to overcome major technological gaps. Others, like the one presented here, involve minor technological improvements that are made within the framework of

conventional ballistics. In this class we shall mention two schemes that are related to ours. Both are based on a dual-stage operation.

The first one is the traveling charge (TC) method originally described by Langweiler² during World War II. The TC concept tries to overcome rarefaction by attaching a second, very fast burning solid propellant charge to the projectile base. The TC is to be ignited after the main charge has almost exhausted its potential to accelerate the projectile and the pressure at the projectile base has dropped. The TC will then burn like a rocket, giving the projectile additional thrust.

Extensive efforts have been made in several laboratories to realize this idea (a recent comprehensive review of the subject is given in Ref. 3). Two main problems exist:

- 1) The TC propellant requires a very high burning rate in order to burn completely, prior to the exit of the projectile from the muzzle. Such propellants gave low reproducibility.
- 2) It is very difficult to control the ignition moment of the TC. Fluctuations in the ignition timing resulted in a wide spread of the muzzle velocities. These severe inherent difficulties have led to inconclusive results, and the prospects of realizing the TC concept remains doubtful.

Another dual-stage gun concept is the light-gas-gun, where a conventional charge accelerates a massive projectile, which compresses an inert light gas to high pressures. The light gas, in turn, accelerates a low-mass projectile. Due to its light molecular mass the light gas has a high speed of sound, hence it is capable of accelerating efficiently the projectile to hypervelocity. Velocities of the order of 10 km/s have been reached in this technique using projectiles having a mass of the order of 1 g. The light-gas-gun has proven to be of great scientific value, yet it is far from being a real candidate for an operative weapon system.

A third dual-stage concept named wave gun⁴ was brought to our attention by the referee. However, further information was not available to us.

In this article we describe a novel dual-stage gun concept which bears some resemblance to the previously described concepts, yet, it has its own unique features that may allow it to be successfully implemented. In this scheme, which we refer as the dual-stage dynamic breech (DSDB) gun, two solid grain propellants are placed in the breech in tandem. The two propellants are separated by a massive buffer that serves as a dynamic breech. We expect this method to allow the acceleration of relatively heavy projectiles to velocities in the range of 2.5–3 km/s. This can be done by minor changes on conventional guns.

Naturally, our scheme has its problems, but as our preliminary experimental results show, they are less difficult to solve.

Received Sept. 16, 1991; revision received March 24, 1993; accepted for publication July 19, 1993. Copyright © 1993 by the American Institute of Aeronautics and Astronautics, Inc. All rights reserved.

*Propulsion Physics Laboratory; currently Department of Electronics, Weizmann Inst. of Science, Rehovot, Israel.

In Sec. II we describe the scheme and discuss its possible advantages and problems. Section III describes a simulation code that has been developed and its predictions. Experiments performed on a test-bed of a 13-mm-diam barrel are described in Sec. IV. Finally, in Sec. V, the conclusions and future research possibilities are presented.

II. Principles of Operation

The basic configuration of the gun is presented in Fig. 1. Two conventional solid grain propellants are sequentially used to accelerate the projectile in two stages. The first stage is purely conventional. The second-stage charge, termed moving charge (MC), is encapsulated in a sealed case attached to the projectile base and stays inert while the first charge accelerates the combined MC and projectile along the initial part of the barrel. At a certain predetermined position or timing, the MC is ignited, creates a large pressure immediately behind the projectile, and accelerates it along the final part of the barrel.

An important role is played by the mass of the MC case in the dynamics of our system. The case separates the volume between the breech and the projectile into two different chambers. The motion of the case is determined by the pressure difference between the two chambers.

While the case's mass is an extra load during the first stage of the acceleration, and can thus be regarded as an unnecessary burden, it serves a good purpose during the second-stage operation. When the MC is ignited, the case's inertia prevents the MC from quickly expanding. Thus, quick and efficient burning of the propellant can be achieved, resulting in the production of a high pressure. This favorable situation would not have occurred if the MC had the possibility to expand freely into the lower pressure gas behind. Later, the case is decelerated by the MC gas. If the case mass is chosen properly, the case reaches the muzzle with diminished velocity, i.e., not much energy is delivered to this parasitic mass. Therefore, from the viewpoint of the MC stage, the MC case functions as a dynamic breech (DB).

The DB must be massive enough so its inertia may confine the MC while it burns. But, on the other hand, it ought to be light enough in order to let the first stage accelerate the system.

The overall dependence of the acceleration process on the DB mass was investigated in the simulations. It was found that the dependence on the DB mass is weak.

At the time of the MC ignition, the projectile is already in motion at a high speed. The time left for the completion of the MC burning and the subsequent expansion of the propelling gas is, therefore, short. Consequently, a very fast gas generation rate is required. In our scheme this high rate is achieved due both to the large surface area of the propellant grains and to the fast burning rate. Thus, the need of an exotic very high burning rate (VHBR) propellant that is necessary for the TC scheme is eliminated.

The timely ignition of the MC is of prime importance for a correct and efficient acceleration process, and the majority of the experimental development effort was dedicated to this

end. As will be shown in the simulations, premature ignition can lead to the development of high pressures in both charges, which might cause the damage to the barrel. Furthermore, the overall efficiency is reduced relative to the properly synchronized process. Late ignition, on the other hand, may result in an incomplete burning of the MC, and therefore lower the total efficiency. Between these two extremes there exists an optimal ignition location that maximized the efficiency of the overall process, i.e., results in a maximal muzzle velocity. This optimum is, however, quite broad due to the interplay between the two acceleration stages, as will be shown in the following section (this behavior was also observed in the experiments, although no systematic work has been done yet in this direction).

Two goals have to be achieved in order to get a proper timing of the MC ignition: 1) the MC case has to be well sealed at all times, to prevent any possible contact between the MC and the hot gas that is produced by the main stage; and 2) a reliable ignition system has to be developed that will ignite the MC at the proper instance.

In order to achieve the first goal, special care has to be given to the longitudinal strength of the case. Since the case is located between the high-pressure gas of the main charge and the projectile, it has to transmit the force from the former to the latter. If not properly designed, the case will yield to the resulting longitudinal stress. Cracks will soon develop that will allow leakage of hot gas into the case and premature ignition will be inevitable.

Ignition of the moving charge can be achieved in several possible ways. An ignitor can be placed inside the moving charge. The ignition signal can either come from a transmitter fixed on the barrel, in the required position, or calculated by an electronic circuit inside the moving charge. The timing in this case can be determined either by counting time from the ignition of the main charge or by integrating twice on the output of an accelerometer.

Although such methods may be the best way to achieve controlled ignition in a real size ammunition, they divert considerable efforts to the development of a smart ignitor. Such efforts are not required for our small scale, proof-of-concept demonstration experiment, where we use another technique that may prove advantageous by itself. It is based on the injection of an intense plasma jet into the moving charge. The plasma jet is produced by a capillary discharge as described in Ref. 5. The plasma injector is placed perpendicular to the barrel. The plasma jet pierces the case and ignites the moving charge.

Precise injection timing is achieved by real-time detection of the arrival of the projectile to the vicinity of the plasma injector. This is done using a threshold detector on the output of a piezoelectric pressure gauge. When the projectile passes the pressure gauge, located a few centimeters before the plasma injector, the pressure in the gauge suddenly rises and the threshold detector issues an activation signal. A short time delay, calculated from the geometrical constants and the predicted projectile velocity, is added to this signal, which then starts the plasma injection. Since the MC has a finite size, the probability that the plasma jet will miss the MC is negligible, even for large deviations from the expected projectile velocity.

III. Simulation

A computer code was written in order to simulate the DSDB gun. We used a lumped-parameter model (zero-dimensional) and assumed the Lagrange model in order to calculate the pressure profiles along the barrel. The specific system that was simulated includes two conventional propellant charges both ignited by plasma injection. We deliberately used small amounts of plasma in order to minimize any possible differences between the simulated system and other systems (e.g., employing other types of ignitors) which are due to the nature of the plasma—propellant interaction.

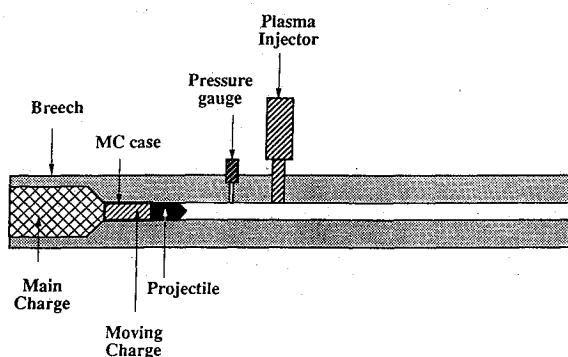


Fig. 1 Schematic description of the dual-stage gun system.

A. Model Equations

In accordance with the general dual-stage nature of the scheme, the simulation is also divided into two stages: before MC ignition (stage 1), and after MC ignition (stage 2). The first stage is basically a conventional one, and it is simulated as such.⁶ Ignition energy is very small, and therefore the exact way in which we are treating ignition is not unequivocal.

In the second stage we assume that the entire mass of the MC case is concentrated in the DB, located between the MC and the gas of the main charge. The dynamics of the DB and the projectile is calculated using the pressure difference between their two sides. The pressures are calculated using adjusted versions of standard models and assumptions that are common in internal ballistic simulations.

In the following paragraphs we discuss the main features of the model.

1. Propellant Burning and Ignition

For the propellant burning we use the conventional, exponential form

$$\dot{x} = b \times p^n \quad (1)$$

where \dot{x} is the rate of regression of the grain surface, and p is the average pressure. The parameters b and n are obtained from the literature or from closed bomb experiments.

We assume that the plasma ignition does not alter the burning rate equation and that the temperature dependence is weak. We treat the injection of plasma into the propellant as an injection of mass and energy which does not alter the properties of the propellant (e.g., its equation of state). This assumption is justified by the small mass of the injected plasma (typically less than 1% of the total mass) and its rapid distribution in the volume.

This set of assumptions is used in the simulation of single-stage, plasma-ignited propellant experiments. Good agreement is obtained between simulation and experimental results.⁷

2. Equations of Motion

Here, we use Newton's second law resulting in

$$a_1 = A \times \frac{P_{1b} - P_{air}}{m_1 + m_2 + C_2} \quad (2)$$

for the acceleration of the whole system during the first stage, and

$$\begin{aligned} a_1 &= A \times \frac{P_{1b} - P_{2c}}{m_1} \\ a_2 &= A \times \frac{P_{2b} - P_{air}}{m_2} \end{aligned} \quad (3)$$

for the acceleration of the two masses during the second stage. Note that the total load mass for the first stage includes the masses of the projectile, the MC, and the DB. Motion starts only when the projectile base pressure is higher than the static friction per unit cross-sectional area, which is taken to be 5 MPa. The transition from joint motion of the projectile and the MC to separated motion occurs when the condition $a_2 > a_1$ is satisfied. As we show later [in Eq. (9)], when the two masses move separately, a connection exists between P_{1b} and P_{2c} . This connection makes the transition into separated motion a little more complicated than it seems at first glance. In some systems this transition may take a considerable time to occur after the ignition of the MC, since the MC has to build enough pressure.

Air pressure in front of the projectile is taken from Ref. 8.

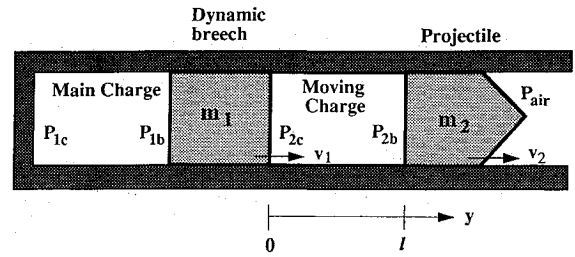


Fig. 2 Schematic description of the dual-stage gun dynamics.

3. Thermodynamics and the Equation-of-State

The gas average pressure is determined by

$$P = \frac{(\gamma - 1)E}{V_g - m_g \eta} \quad (4)$$

where E is the total gas internal energy, γ is the ratio of specific heats, V_g is the gas volume (the total volume minus the volume occupied by the solid propellant), m_g is the gas mass, and η is known as the covolume per unit mass.

The gas temperature is calculated using the well known Abel-Nobel equation-of-state which is customary in internal ballistics calculations

$$P(V_g - m_g \eta) = nRT \quad (5)$$

where R is the gas constant and n is the number of gas moles.

The ratio of specific heats and the covolume are usually supplied by the propellant's producer, and are typically 1.25 and $1.1 \times 10^{-3} \text{ m}^3/\text{kg}$, respectively.

Heat losses to the barrel are obtained from the Nordheim model,⁹ using an experimentally matched heat transfer factor of 0.3 for the 60-mm gun and 0.8 for the 13-mm gun.

4. Pressure Profile Along the Barrel

Since we use a lumped parameter model (zero-dimensional), we need a way to calculate—at least approximately—the pressure profile along the barrel axis. The simplest and most widely used model is the Lagrange model,¹⁰ which assumes a constant density along the barrel. Let us extend this model to a more general case of a gas enclosed between two moving masses, as shown in Fig. 2.

Using the continuity equation in one dimension and the Lagrange assumption ($\rho = \text{const}$) we obtain that at any given moment the velocity profile is linear. Using the boundary conditions at both ends of the gas column we obtain the following velocity profile:

$$v(y) = v_1 \left(1 - \frac{y}{l}\right) + v_2 \frac{y}{l} \quad (6)$$

where the y axis is directed along the barrel's axis from m_1 , and l is the total length of the gas column. The pressure profile can be found using the Euler (force) equation

$$\frac{\partial P}{\partial y} = -\rho v \quad (7)$$

and the acceleration of the bodies, as given by Newton's law in Eq. (3).

Combining Eqs. (3), (6), and (7), integrating for $P(y)$, and using the boundary condition $P(0) = P_{2c}$, we find

$$\begin{aligned} P(y) &= P_{2c} - C_2 \times \left\{ \frac{P_{1b} - P_{2c}}{m_1} \times \left[\frac{y}{l} - \frac{1}{2} \left(\frac{y}{l} \right)^2 \right] \right. \\ &\quad \left. + \frac{P_{2b} - P_{air}}{m_2} \times \frac{1}{2} \left(\frac{y}{l} \right)^2 \right\} \end{aligned} \quad (8)$$

We can now use this result to find an expression for P_{2b} by substituting $y = l$, and an expression for P_2 by integrating over y and dividing by l . From these expressions we can finally extract expressions for P_{2b} and P_{2c} as a function of P_2 , P_{air} , and P_{1b} .

The results are

$$\begin{aligned} P_{2b} &= P_2 \times \frac{1}{I_1} + P_{air} \times \frac{J_1}{I_1} + P_{1b} \times \frac{K_1}{I_1} \\ P_{2c} &= P_2 \times \frac{1}{I_2} + P_{air} \times \frac{J_2}{I_2} + P_{1b} \times \frac{K_2}{I_2} \end{aligned} \quad (9)$$

where

$$\begin{aligned} I_1 &= \frac{1 + \phi}{2} + \frac{C}{m_2} \frac{1 + 3\phi}{12} \\ I_2 &= \frac{1 + \theta}{2} + \frac{C}{m_1} \frac{1 + 3\theta}{12} \end{aligned} \quad (10)$$

$$\begin{aligned} J_1 &= \frac{C_2}{m_2} \frac{1 + 3\phi}{12} \\ J_2 &= \frac{C_2}{m_2} \frac{1 - 3\theta}{12} \end{aligned} \quad (11)$$

$$\begin{aligned} K_1 &= \frac{C_2}{m_1} \frac{1 - 3\phi}{12} \\ K_2 &= \frac{C_2}{m_1} \frac{1 + 3\theta}{12} \end{aligned} \quad (12)$$

$$\begin{aligned} \theta &= \frac{1 + (C_2/6m_2)}{1 + (C/2m_2)} \\ \phi &= \frac{1 + (C_2/6m_1)}{1 + (C/2m_1)} \end{aligned} \quad (13)$$

This general result can readily be reduced to the case of a single-stage, static breech gun. Using the appropriate replacements: $C_2 \rightarrow C$, $m_2 \rightarrow m$, $m_1 \rightarrow \infty$, $P_{air} \rightarrow 0$, $P_{1b} \rightarrow 0$, $P_{2b} \rightarrow P_b$, and $P_{2c} \rightarrow P_c$, we obtain the known Lagrange expressions:

$$\begin{aligned} P_b &= P \times \frac{1}{1 + (C/3m)} \\ P_c &= P \times \frac{1 + (C/2m)}{1 + (C/3m)} \end{aligned} \quad (14)$$

Using similar replacements we also found expressions for P_{1b} and P_{1c} in the case of a dual-stage gun. These expressions are used in the simulation and establish a coupling between the two gas media. Note that the coupling parameters $I_{1,2}$, $K_{1,2}$ depend only on mass ratios. These parameters are constant throughout the ballistic process and do not depend on the velocity.

The use of the Lagrange assumption of a constant density is justified in the same way as in normal gun simulations where the Lagrange model is extensively used: it is simple and it works fine when simulations are compared to experiment in a wide range of systems. In our case, the situation is much more complicated than in a single-stage gun, hence, any attempt to go beyond this simple approach will require very complicated one-dimensional simulations which are beyond the scope of this work.

Qualitatively, this model correctly accounts for the interplay between the two gas media. For example, as the MC is ignited and the two masses start moving with different accelerations, a compression wave is observed, starting at the dynamic breech base. The compression is due to the fact that the dynamic breech is decelerated while the rear stage gas

tends to inertially continue at its former velocity. This effect is accounted for in our equations.

Finally, the reasonable agreement between our experiment and the simulation, as shown in Fig. 11, indicates that in our case the approximation is not very crude.

B. Simulation Results

Simulation of a MC experiment on a 60-mm gun was performed. This type of gun is presently the main technology test-bed in our laboratory. The system parameters used in this simulation are shown in Table 1.

Simulated average pressure curves, in both chambers, as a function of time are shown in Fig. 3. The projectile's velocity at the ignition of the MC was 1400 m/s and the muzzle velocity was 2595 m/s. As can be seen from the figure, the peak pressures of both stages is kept below 500 MPa, the barrel's maximum pressure (in the main charge the breech pressure, which is not shown, reaches 500 MPa). In Fig. 4 the projectile velocity curve along with the dynamic breech velocity are presented.

In this figure we also give, for comparison, the velocity curve in a case where the MC was not ignited (i.e., a conventional shot with a heavier projectile of mass $m_t = m_1 + m_2 + C_2$). As a reference, we also show in the same figure the velocity curve in an equivalent, optimized single-stage shot. The reference shot uses the same barrel and projectile parameters, the same propellant with optimized dimensions, the same total energy input, and an optimized initial volume. The muzzle velocity in the reference shot was 2160 m/s, slower by 435 m/s than the optimized MC shot.

Table 1 Simulation parameters for 60-mm MC gun

Barrel diameter	60 mm
Barrel length	4.4 m
Projectile travel	4.0 m
Projectile mass	0.48 kg
Dynamic breech mass	0.3 kg
Main charge mass	1.6 kg
Main charge propellant	M30P7 ($L = 8$, $D = 3.5$, $d = 0.15$ mm)
MC mass	465 g
MC propellant	Winchester 860 (ball, $D = 0.74$ mm)
Chamber volume	2260 cc
MC volume	500 cc
Ignition location	2.2 m (from breech)
Ignition energy, main	200 kJ @ 0.5 ms
Ignition energy, MC	250 kJ @ 0.25 ms
Peak pressure, main	500 MPa
Peak pressure, MC	500 MPa
Muzzle velocity	2595 m/s

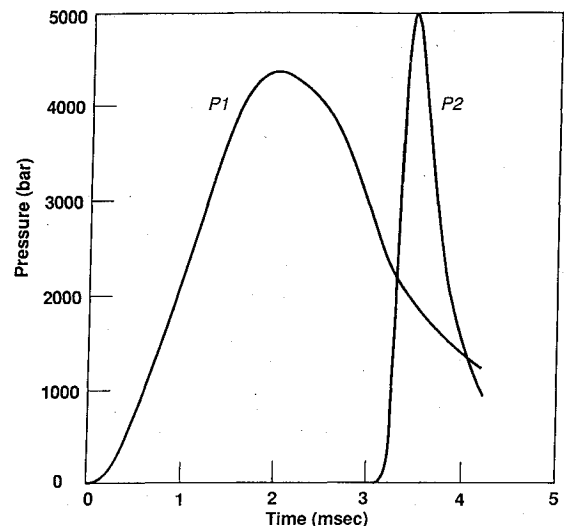


Fig. 3 Simulation results: average pressure curves in the two chambers. Run parameters are given in Table 1.

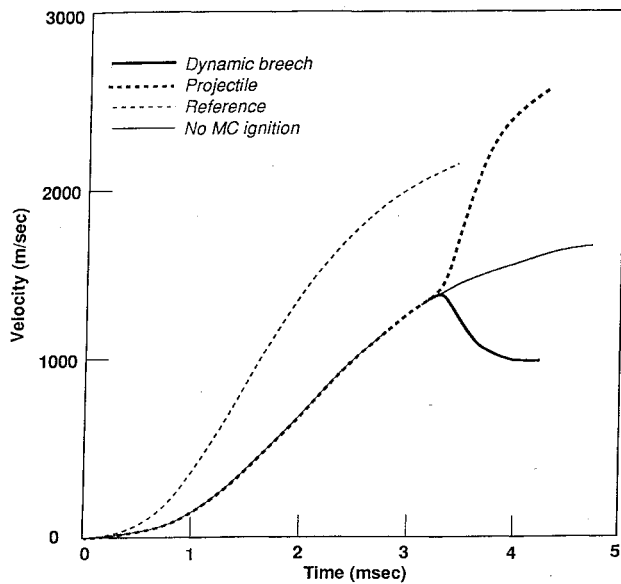


Fig. 4 Velocity curves of the projectile and the dynamic breech for the same run shown in Fig. 3. Also shown is the velocity for the case that the MC is not ignited, and a reference velocity curve of an optimized conventional run (see text).

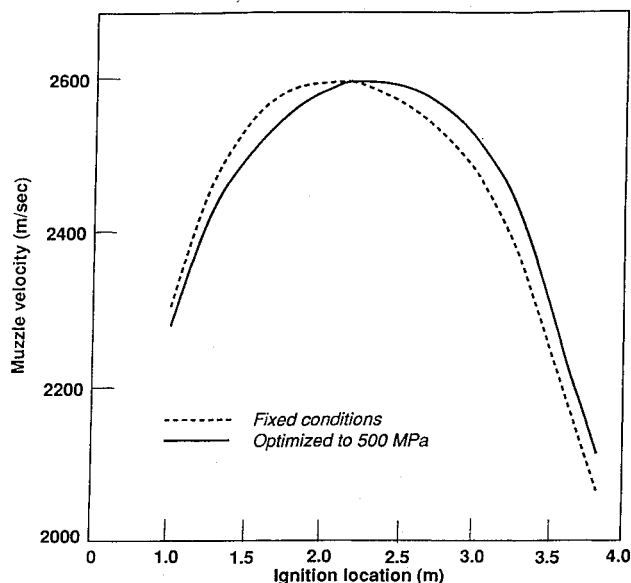


Fig. 5 Simulation results: muzzle velocity dependence on the ignition location.

In Fig. 5 we show the dependence of the acceleration process on the ignition location. Each point on the curve gives the result of a run that is optimized for a given ignition location. The optimization was done by varying only the charge weights, keeping all other parameters constant. The peak pressures in all optimized runs were 500 ± 0.5 MPa. The reason for the existence of an optimum ignition location is the competing effects that the ignition location has on the two stages, as discussed previously. The simulation shows that this optimum is quite insensitive, over a wide range, to the ignition location: we can change the ignition location by as much as ± 0.5 m and lose only 35 m/s from the optimum velocity. The second curve also shows the dependence on ignition location, but this time without any optimization: the same system, with the same charges, is ignited at different locations. The results tend to be higher at ignition locations closer to the breech and lower farther away from the breech. However, the main behavior is the same and the dependence is not very strong. In these runs, peak pressures were not limited and the MC

peak pressure was higher than 500 MPa for ignition locations shorter than 2.2 m.

In Fig. 6 we show the dependence of the muzzle velocity on the dynamic breech mass. Similar to Fig. 5, one curve represents the simulation of the same system varying only the dynamic breech mass, whereas in the other curve, an optimization was done for each mass separately, varying the propellant charges and keeping the pressures within 500 ± 0.5 MPa. As can be seen from the figures, while the total accelerated mass, $m_t = m_1 + C_2 + m_2$, changes by a factor of 2 the muzzle velocity is reduced only by about 8%. This weak dependence is due to the positive effect of the dynamic breech mass on the MC stage. Again, in the unoptimized curve the pressures are higher than 500 MPa for $m_1 > 0.3$ kg, resulting in higher velocities than in the optimized case.

IV. Experiments

We present the results of a proof-of-concept experiment on the 13-mm-diam, 1-m-long barrel. The experimental setup is shown in Fig. 7. The main experimental effort was dedicated to the development of a controlled, reliable ignition method, since this is the key to the successful implementation of the dual-stage gun. Dual-stage operation was repeatedly demonstrated and studied. In these experiments we used the plasma ignition method, and the plasma jet source was a capillary discharge injector.⁵ In this method the MC case has to conform to two requirements that are usually contradictory: 1) it has to prevent premature ignition of the MC and 2) it has

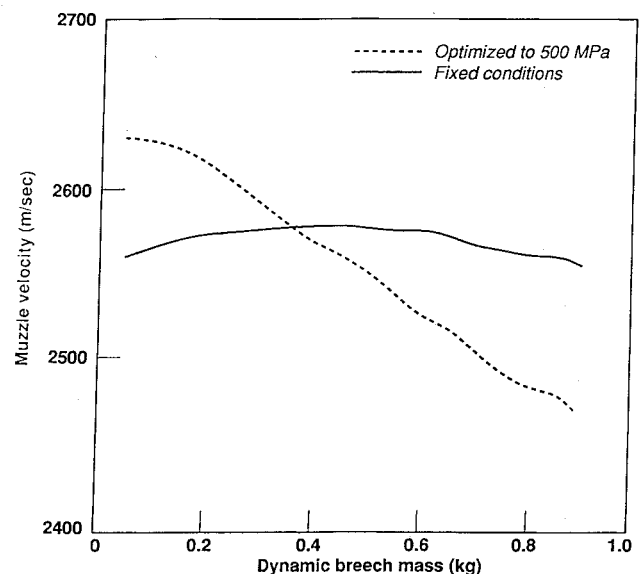


Fig. 6 Simulation results: muzzle velocity dependence on the dynamic breech mass.

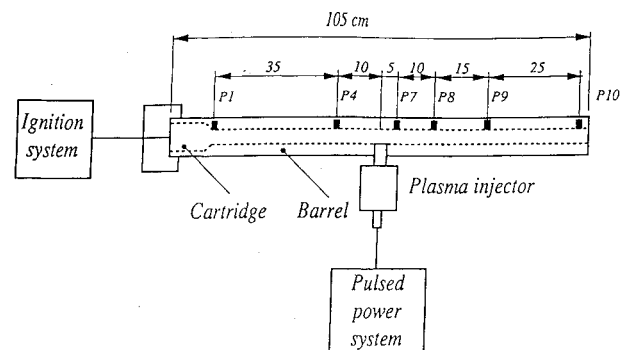


Fig. 7 Experimental setup on a 1-m-long, 13-mm-diam barrel. The locations of several Kistler pressure gauges and the ignition plasma injector are indicated.

to allow controlled ignition using the plasma jet. These conflicting requirements impose stringent limitations on the design of the MC case.

Premature ignition occurs when hot gases from the main charge reach the MC. In order to avoid such contact it is necessary to ensure good sealing of the MC case. However, sealing is not enough since the MC case is placed under a heavy longitudinal stress when the system accelerates. If the case is not strong enough to withstand this stress, cracks soon result, the case breaks down and any small amount of hot gas will cause premature ignition. However, if the case is made too strong, it might not allow the plasma jet to penetrate and ignition would not be achieved at all.

The design we have implemented is shown in Fig. 8. This design includes a threaded polycarbonate case, which encloses the MC and prevents any contact between the MC and blowby hot gases from the main charge. The copper seal serves to keep blowby to the MC area to a minimum. The projectile is designed such that its rear part, the spine, is in direct contact with the copper seal. Such contact allows direct momentum transfer from the seal to the projectile during first-stage acceleration, significantly reducing the longitudinal stress on the polycarbonate case. Note that the projectile was not optimized as far as intermediate or terminal ballistics are concerned. This design successfully prevented premature ignition in a large number of shots while allowing the plasma jet to pierce through the case and ignite the MC.

In our experiments the first acceleration stage was not conventional, but an electrothermal (ET) acceleration process,¹¹ using water as the working fluid. This difference is of no significant importance since our main interest is in the controlled operation of the MC stage, and we believe that a similar experiment can be performed, with equal success, using a conventional first stage. The ET stage was not optimized, and we know from other experiments that in the configuration used the typical efficiency of the process is only about 20%, much lower than that of conventional acceleration. The parameters of a typical experiment are listed in Table 2.

Understanding of the process is gained by looking at the pressure curves measured by the gauges distributed along the

Table 2 Experimental parameters for the 13-mm dual-stage gun

Barrel diameter	13 mm
Barrel length	1.15 m
Projectile travel	1.05 m
Projectile mass	36 g
Copper seal mass	26 g
MC case mass	12 g
Water mass	6 g
MC mass	7.4 g
MC propellant	Winchester 860 and 231 (ball $D = 0.74$ mm)
Chamber volume	16 cc
MC volume	8 cc
Ignition location	0.55 m (from breech)
ET energy	44 kJ @ 1.0 ms
MC ignition energy	9.4 kJ @ 0.1 ms
Peak pressure, main	360 MPa
Peak pressure, MC	≥ 550 MPa
Muzzle velocity	1070 m/s

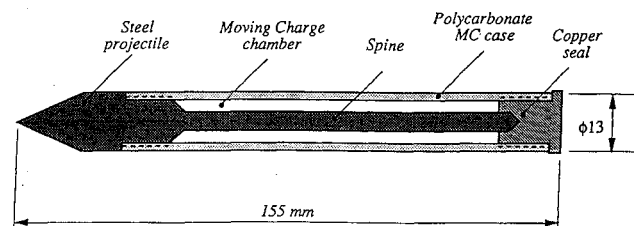


Fig. 8 Sample integrated projectile design for 13-mm barrel experiments, using a metal spine to prevent longitudinal breakdown. The copper seal significantly reduces gas blowby to the MC. (Design considerations did not include external or terminal ballistics.)

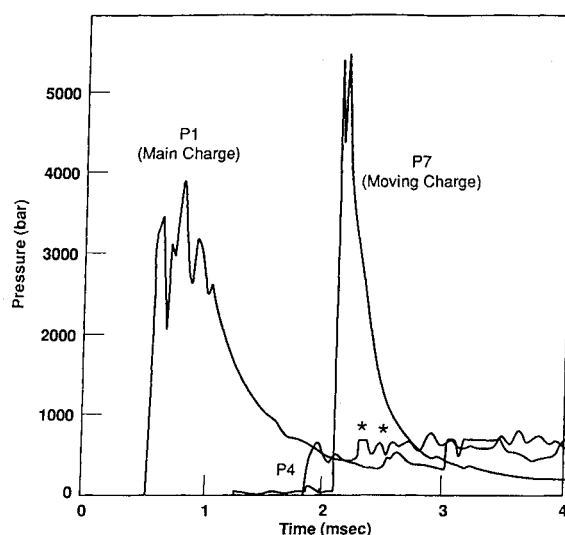


Fig. 9 Experimental results: pressure curves measured in the main charge (P1), prior to the plasma injector (P4) and in the TC (P7). * indicates the appearance of a compression wave as the dynamic breach is decelerated.

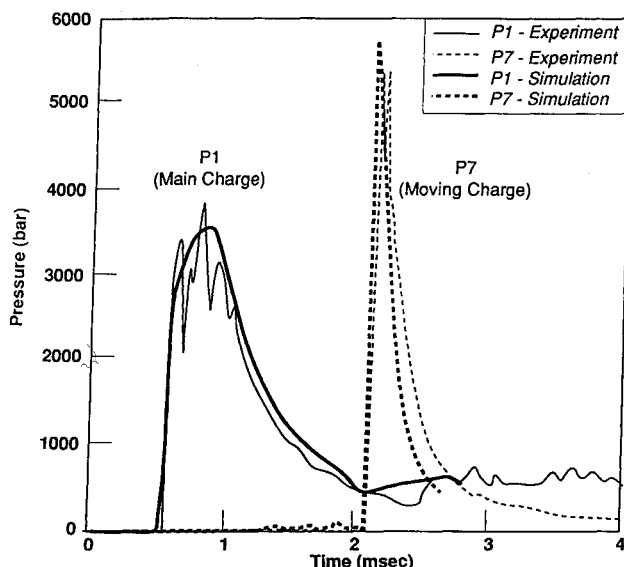


Fig. 10 Experimental results: pressure curves measured on the gauges P7-P10. The curves of P8-P10 are shifted downward for clarity. * indicates the secondary peak which is due to the passage of the dynamic breach.

barrel, as shown in Fig. 7. Pressure curves from a typical shot are shown in Figs. 9 and 10. From the measured pressure curves we can reconstruct the pressure profile along the barrel and the locations of the projectile and the DB at different times.

The pressure curve measured in P1 is that of the first stage and it does not show any interesting features prior to 2-ms time. The irregular peaks are a result of the uncontrolled nature of the plasma-fluid mixing in the ET gun, and also appear in single-stage ET shots. The high pressures measured by the P7 pressure gauge, 5-cm downstream from the plasma injector, prove that the MC was indeed ignited on time. Other pressure gauges located farther downstream from the plasma injector also show exceptionally high pressures, much higher than the ones measured close to the breech at the same time. These high pressures are the result of the ignition of the MC. Looking at P1 and P4 we can see a compression wave heading backward, after ignition of the MC, which is the result of the deceleration of the dynamic breach. At later times we can also trace the motion of the dynamic breach on P7-P10 as a

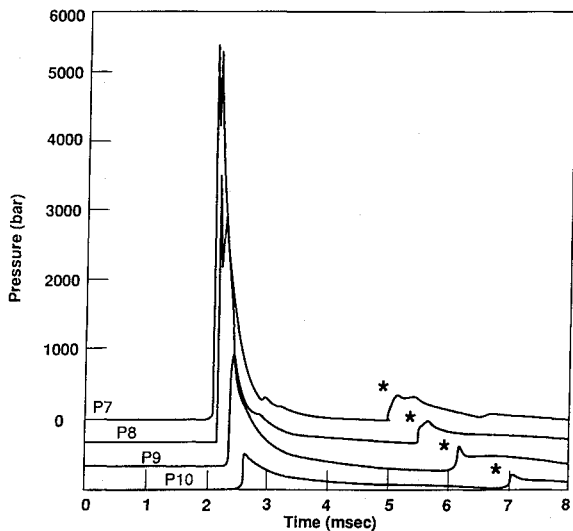


Fig. 11 Simulation and experimental results on 13-mm barrel: pressure curves measured on gauges P1 and P7.

secondary pressure pulse. These pulses allow us to measure the muzzle velocity of the dynamic breech.

The projectile muzzle velocity in this experiment was 1070 m/s, almost twice the velocity measured in a reference experiment in which the MC was not ignited. The projectile kinetic energy was 20 kJ and the overall efficiency was 24%. This relatively low figure can be largely attributed to the low efficiency of the first ET stage and the large heat losses typical to small caliber guns. The DB velocity measured was 300 m/s, amounting to a kinetic energy of only 1.4% of the total input energy.

In Fig. 11 we show the result of a simulation run that closely reconstructs the measurements of P1 and P7 and the measured projectile velocity. The simulation uses the available experimental parameters. However, three parameters—friction and the two MC burning rate coefficients—were varied in order to well reproduce the experimental data. We had to use this procedure because of the lack of reliable data for the fast propellant. The first, electrothermal stage is taken in an approximate way as the burning of a nonenergetic propellant that completes its burning at the end of the injected plasma pulse.

V. Conclusions

We have presented a novel acceleration scheme based on the successive operation of two conventional propellant charges. The main charge can be fully conventional (or other), while the second stage charge is carried behind the projectile, in a suitable casing, and is ignited only at a later time.

The second—or MC—is placed close to the projectile base, thus avoiding the rarefaction effect and increasing the efficiency over conventional ballistics. The additional parameters of this scheme allow many new degrees of freedom (DOF) and thus an optimization of the process can yield better results.

A zero-dimensional simulation code of the ballistic process was written using conventional assumptions. An expanded version of the Lagrange model was developed in order to account for the pressure profile between two moving masses in the barrel. The dependence of the muzzle velocity on the ignition location and on the dynamic breech mass was investigated. We found that an optimum ignition location existed,

allowing the first stage to be well exploited prior to the ignition of the MC, and giving the MC stage enough time to burn out completely and transfer its energy to the projectile. The simulation shows weak dependence of the velocity on the ignition location, therefore making its accurate determination less important than in other dual-stage schemes. The dependence of the muzzle velocity on the dynamic breech mass was found to be weak as well.

The simulation of a particular system shows that a 0.48-kg projectile can be accelerated to beyond 2500 m/s on a 4.4-m-long, 60-mm gun, compared to a maximum of ≈ 2160 m/s that can be achieved using conventional ballistics with similar pressure restrictions.

In a proof-of-concept experiment on a 1-m-long, 13-mm-diam barrel we have demonstrated controlled MC ignition and the expected dynamics of a dual-stage gun. The use of off-the-shelf propellants and the good timing control allows for reliable operation of the presented design.

Upgrading of the experiment to larger calibers may allow us to demonstrate acceleration to hypervelocities using this scheme. In larger caliber guns we would be able to utilize several ignition and casing techniques that were impossible to apply at the small scale of the present experiments.

The appearance of significant wave phenomena due to the ignition of the MC obviously calls for at least a one-dimensional simulation, since the lumped-parameter simulation presented can only crudely take these effects into account.

Acknowledgments

The authors would like to thank Y. Oreg, D. Melnik, J. Ashkenazi, D. Saphier, and Z. Goralik for fruitful discussions. The technical assistance of S. Arie, Y. Gerasi, Z. Zeevi, G. Appelbaum, and M. Melnik is also highly appreciated. We are greatly indebted to N. Spector for useful discussions and suggestions.

References

- ¹Rashleigh, C. S., and Marshall, R. A., "Electromagnetic Acceleration of Macroparticles to High Velocities," *Journal of Applied Physics*, Vol. 49, No. 4, 1978, pp. 2590–2592.
- ²Langweiler, H., "A Proposal for Increasing the Performance of Weapons by the Correct Burning of Propellant, Impulse Propulsion," Wa Pruef 1/IIb, Berlin, 1939, Trans. British Intelligence Objective Sub-Committee, Group 2, Ft. Halstead Exploiting Center, Rept. 1247, UK, 1945.
- ³Baer, P. G., and May, I. W., "Traveling Charge Effect," *Gun Propulsion Technology*, edited by L. Stiefel, Vol. 109, Progress in Astronautics and Aeronautics, AIAA, Washington, DC, 1988, Chap. 15.
- ⁴Astron Corp., Internal Rept.
- ⁵Loeb, A., and Kaplan, Z., "Methodology of Capillary Discharge," *IEEE Trans. Mag.*, Vol. 25, No. 1, 1990, pp. 342–346.
- ⁶Krier, H., and Summerfield, M., "Interior Ballistics of Guns," Vol. 66, Progress in Astronautics and Aeronautics, AIAA, New York, 1979.
- ⁷Brill, B., Wald, S., and Kaplan, Z., "Hybrid Plasma-Propellant Acceleration of Projectiles to Hypervelocities" (to be published).
- ⁸Celmins, A. K., "Modeling of Recoilless Rifle Ballistics," *Interior Ballistics of Guns*, H. Krier and M. Summerfield, New York, 1979, pp. 113–134.
- ⁹Baer, P. G., "Practical Interior Ballistic Analysis of Guns," *Interior Ballistics of Guns*, H. Krier and M. Summerfield, New York, 1979, pp. 37–66.
- ¹⁰Corner, J., *Theory of the Interior Ballistics of Guns*, Wiley, New York, 1950.
- ¹¹Metzgar, T. L., "Electrothermal Guns: The Next Step on the Road to Hypervelocity," National Defence, Sept. 1990, pp. 20–23.